

# EFFECTS OF WETTABILITY AND INTERFACIAL TENSION ON THE DISTRIBUTION OF RESIDUAL OIL ON THE PORE SCALE AFTER WATER FLOODING

T. Ramstad<sup>1,2</sup>, T. Varslot<sup>2</sup>, R. Meland<sup>2</sup> and O. J. Arntzen<sup>1</sup>

<sup>1</sup>Statoil RDI, Trondheim, Norway

<sup>2</sup>FEI Lithicon Digital Rock Services, Trondheim, Norway

*This paper was prepared for presentation at the International Symposium of the Society of Core Analysts held in Avignon, France, 8-11 September, 2014.*

## ABSTRACT

We have performed numerical pore scale simulations and detailed analysis of the resulting configuration, distribution and amount of residual oil in the pore space of a reservoir rock during and after water-flooding. The simulations were performed using a multiphase lattice-Boltzmann (LB) solver on a digital rock model which had been constructed from high-resolution 3D micro-CT images. The micro-CT images were acquired from a sandstone reservoir. Using this type of simulation it is possible to follow and map fluid configurations during displacement in detail, and thus analyze and quantify the fluid distributions inside the pores. In our study we looked at both water wet and intermediate wet conditions, each of which was simulated for four different interfacial tensions, giving rise to a total of eight simulated cases. In each case the final residual oil configuration was recorded after injecting approximately three pore volumes (PV) of water. We then identified individual oil clusters and computed statistics such as cluster length and size distribution. The results indicated that the interfacial tension has a clear impact on the residual oil saturation and configuration. This applies even for intermediate values of interfacial tension, i.e. not only ultra-low values. There are also clear differences between the water wet and the intermediate wet cases in terms of the production curves and oil cluster distribution.

## INTRODUCTION

Although water flooding has been used for decades to recover oil, many questions and uncertainties remain with respect to oil recovery and trapping mechanisms at the pore scale. Wettability and the balance between viscous and capillary forces are major factors controlling the displacement and distribution of fluids in porous rocks, [1].

Several chemical enhanced oil recovery (EOR) techniques have been designed to increase the microscopic displacement efficiency and mobilize trapped oil by altering wettability and interfacial tension. The potential of such EOR methods depend strongly on the distribution of oil in the pore space. This, in turn, is closely linked to the cluster size and length on which a viscous pressure gradient can act [2].

Direct imaging of the fluid distribution, and especially the displacement process in the pore space of reservoir samples is, however, still a challenging task [3]. A complementary approach is to perform numerical simulations of the fluid transport through a digital representation of the pore space obtained from 3D images. With numerical simulation of pore scale flow it is possible to extract information about the *in-situ* fluid distribution and get a better understanding of EOR mechanisms.

The main objective of this work is to study how variations in wettability and interfacial tension (IFT) affect the magnitude and distribution of residual oil in a reservoir rock sample during and after a water-flood. This objective has been achieved through numerical simulations of water flooding in a representative reservoir rock model. The simulated fluid distributions were recorded and analysed both statistically and through qualitative, visual inspections of oil clusters in the pore space.

## **METHOD AND SETUP**

We have simulated two-phase flow on digitized rock microstructure images using a lattice Boltzmann (LB) method. The LB method is a computational fluid dynamics technique that is well suited for simulating two-phase flow in complex geometries, such as rock microstructures. It relies upon a simplified collision and propagation scheme of local fluid distributions, and is able to correctly reproduce macroscopic behaviour and at the same time capture local microscopic effects. For phase separation we utilize a modified color gradient scheme with surface forces directly regulated by the value of the interfacial tension and wettability [4].

The digital 3D rock model used in the simulations is reconstructed from X-ray micro-CT imaging of a reservoir rock sample from a field on the Norwegian Continental Shelf. The sample is a well-sorted, relatively clean and homogeneous sandstone from the Tarbert formation of the BRENT group with a presence of slightly dissolved feldspar and small amounts of mica and pyrite. The approximate content of clay is 4.6 wt.%.

The digital rock model which was used in these simulations was obtained by segmenting a high-resolution micro-CT image of the rock into void pore space and solid matrix. The resolution of the model is 5 microns/voxel and with a total size of 400×400×400 voxels it yields a volume of 8 mm<sup>3</sup>. A generated image of the grid is shown in **Fig 1** with properties listed in **Table 1**.

To study the effects of wettability on the saturation and configuration of remaining oil, we simulated the injection of water at a constant rate for two different contact angles: 30 and 70 degrees, referred to as water wet (WW) and intermediate wet (IW), respectively. For each contact angle, simulations were performed with four different oil-water IFTs: 40, 10, 1 and 0.1 dynes/cm (mN/m).

The ratio between viscous and capillary pressure drop at the pore scale is given by the

capillary number  $Ca = (u\mu)/\sigma$ , where  $u$  is the total flow rate of oil and water,  $\mu$  is the effective dynamic viscosity, and  $\sigma$  is the IFT.

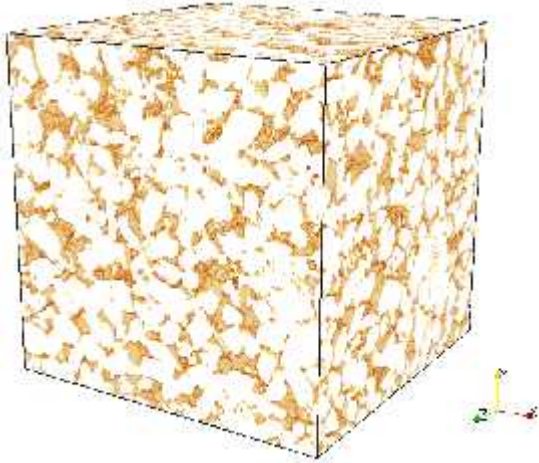


**Figure 1:** Micro-CT image used as basis for the digital rock model

Digital Rock Model		
k (model avg)	(mD)	2567
$\Phi_{(\text{intergranular})}$	(frac.)	0.273
$\Phi_{(\text{tot})}$	(frac.)	0.296
Visc oil	(cPoise)	4.0
Visc water	(cPoise)	0.5
Flow velocity	(m/day)	1.9

**Table 1:** Petrophysical properties of the digital rock model

The configuration of the water flood residual oil was analyzed by calculating the cluster size and length distributions of the residual oil after approximately 3 pore volumes (PV) of water injected.

## RESULTS

All simulations of water injection were started independently and with an initial intergranular water saturation ( $S_{wi}$ ) of 0.05 distributed and relaxed according to wettability to give a uniform saturation profile of  $S_{wi}$ . As shown in **Fig 2** the amount of produced oil increases linearly prior to water breakthrough for both wettability states. For the WW cases the crossover in oil production is sharp after water breakthrough (about 0.5 PV on injected water) and little oil is produced. This is especially the case for higher IFT. The resulting residual oil saturations ( $S_{or}$ ) are clearly dependent on the IFT. For 40 dynes/cm and 10 dynes/cm,  $S_{or}$  has about the same ultimate value. However, the change is profound when going down to 1 dynes/cm and 0.1 dynes/cm.

The residual oil saturations for the IW cases display a similar dependency on IFT. In addition, a significant tail production of oil is observed. This behaviour is consistent with measurements from core flooding experiments [5], suggesting that the residual oil saturation is dependent on the total water throughput to a much larger degree than for the WW samples.

Visual inspection of the residual configuration (**Fig 3**) reveals fundamental differences in the oil distribution for the two wettability states. For the WW case, the oil clusters are rounded in shape, disconnected and occupy the centre of the pore bodies. The IW clusters

form longer and more connected pathways of oil in the pore space. Also, for the IW case, the frequency of very small clusters (fragments) is much higher than for the WW case.

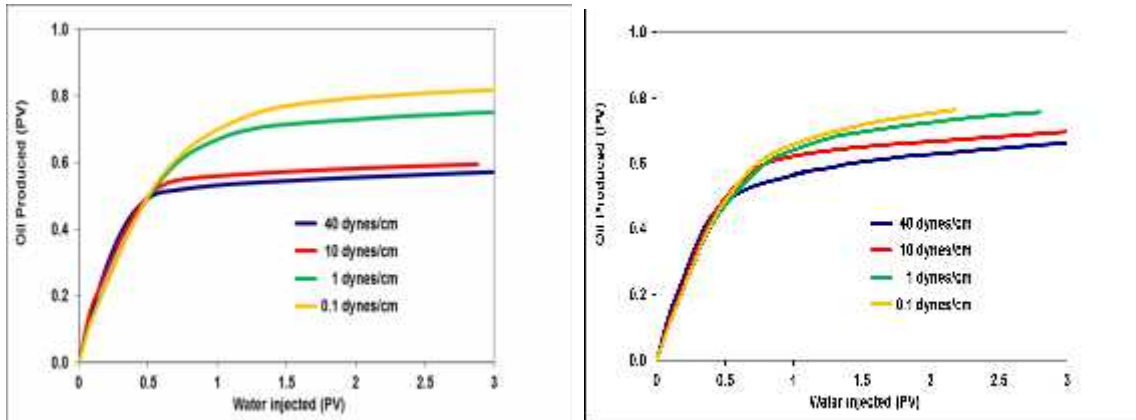


**Figure 2:** Cumulative oil production plotted against amount of injected water for different IFT. WW case left and IW case right.

The low tail production of oil in the WW case can be understood from the way water invades the sample leading to capillary trapping of oil clusters. For flow regimes with high IFTs, larger pores tend to be invaded after the smaller ones. Water prefers to move in the smallest channels and in films. As the thicknesses of the films grow, snap-off occurs at pore throats leaving behind oil clusters in large pores. These are trapped and do not contribute to the oil production. However, for snap-off to occur, a sufficient amount of water must be transported to the snap-off site before the oil is displaced. This transport is essentially driven by capillary pressure differences. This partly explains why the lower IFT cases have a lower residual oil saturation. Capillary pressures are lower and the water transport (imbibition) is not fast enough to execute the snap-off before the oil escapes.

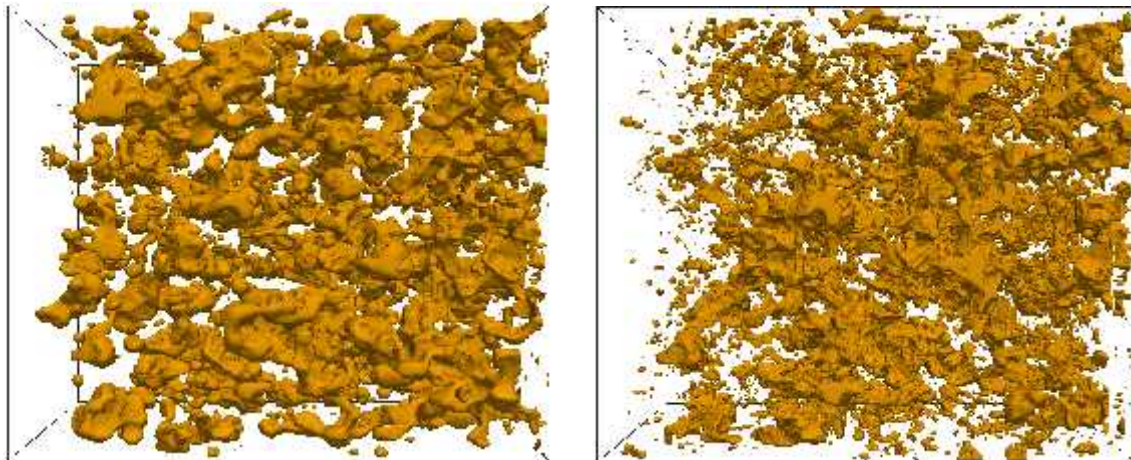


**Figure 3:** Snapshot of residual oil distribution at 40 dynes/cm. WW left, IW right.

The other explanation is that for lower IFT, the larger pores are invaded earlier by water. This leads to a delayed water breakthrough and more oil production. More oil clusters residing in narrow pores and fewer in wide pores remain trapped in these cases.

In the case of IW and increased contact angle, the water preference for smaller pores is reduced. The water will also in this case by-pass oil, but the snap-off effects are less pronounced. In general, with the higher contact angle, snap-off occurs at higher local water saturation. This combined with the fact that the capillary-driven corner flow is reduced in the IW case, suggests that snap-off should be much more rare. The reduced frequency of snap-off and the earlier displacement of oil from larger pores can explain the lower  $S_{or}$  and the higher tail production compared to the WW case.

The effects of water invasion on the residual oil can be examined quantitatively through statistical analysis of the oil cluster distribution. The resulting residual oil saturation and the cumulative distribution of cluster lengths are shown in **Fig 4**. For the cluster distribution curves for the WW case (dotted line) there is a clear cut-off in all curves which suggests that large, spanning oil clusters are not present in the sample [6]. As mentioned, we suggest that this is caused by snap-off processes. As the IFT is reduced, more of the oil is displaced before snap-off can occur. This leads to fewer and shorter oil clusters. The resulting capillary desaturation curve (CDC) for the WW case is in qualitative agreement with previous experimental studies [5].

Plotted in the same figure is the cluster distribution of the IW case (solid line). Here the cut-off is less distinct and clusters of all length scales exist. Compared to the snapshot of the in-situ oil distribution of **Fig 3**, the statistical distribution of oil clusters suggests a reorganization of oil configuration towards long, spanning clusters at the expense of medium sized ones. Such a conclusion is drawn from the size distribution which changes surprisingly little with decreasing IFT. This behaviour will eventually result in a continuous tail production of oil if long oil clusters are sustained.

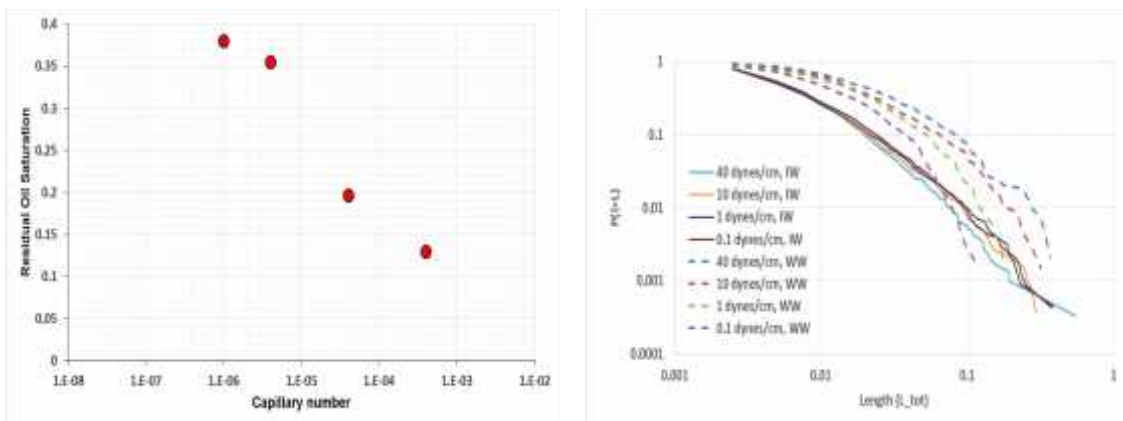


**Figure 4:** Capillary desaturation curve of WW case (right). Cumulative cluster length distribution of WW oil clusters (dotted line) and IW oil clusters (Solid line).

## CONCLUSIONS

IFT and wettability affects the residual oil saturation and distribution also at intermediate values of the IFT.

In the water wet (WW) case snap-off is frequent for the high IFT cases resulting in high  $S_{or}$ . With lower IFT snap-off is less frequent, especially for larger pores, resulting in lower  $S_{or}$ . There is little tail production in the WW case indicating that snap-off to a large degree has occurred before the time of breakthrough. For high IFT residual blobs tend to be larger than for lower IFT. This can be explained by the order in which pores are invaded: When the IFT is high, the small pores are preferentially invaded due to the dominance of capillary forces, leaving isolated clusters of trapped oil in the larger pores. For low IFT, the capillary forces are less dominating, and the large pores are invaded much earlier.

Lowering the IFT results in lower  $S_{or}$  also for the intermediate wet (IW) case, though not to the same degree. Residual oil appears to be more continuous, and we also observe a significant tail production of oil. These observations can be attributed to a reduced frequency of snap-off. Residual cluster size distribution shows little variation with IFT compared to the WW case. This is expected, since in this case the water-flood has much less the character of an imbibition process.

## ACKNOWLEDGEMENTS

The authors acknowledge Statoil RDI for granting permission to publish this paper. We also thank Knut Uleberg for helpful discussions.

## REFERENCES

1. Lake L. W., "Enhanced Oil recovery", Prentice Hall (1989).
2. Armstrong *et al.* "Critical capillary number: Desaturation studied with fast X-ray computed tomography", *Geophysical Research Letters* **41**, 1-6 (2014).
3. Berg S *et al.*, "Multiphase Flow in Porous Rock imaged under dynamic flow conditions with fast X-ray computed micro-tomography", SCA 2013-011 (2013).
4. Ramstad *et al.* "Relative Permeability Calculations from Two-Phase Flow Simulations Directly on Digital Images of Porous Rocks", *Transport in Porous Media* (2012), DOI 10.1007/s11242-011-9877-8.
5. G. Paul Willhite, "Waterflooding", ISBN 978-1-55563-005-8 (1986).
6. Ramstad T and Hansen A, "Cluster evolution in steady state two-phase flow in porous media", *Physical Review E* **73**, 026306 (2006).